Response to Reviewers' Comments amt-2019-141: Estimating Solar Irradiance Using Sky Imagers

Soumyabrata Dev, Florian M. Savoy, Yee Hui Lee, Stefan Winkler

August 10, 2019

We would like to thank the Associate Editor and the anonymous reviewers for your valuable comments and suggestions. Based on your inputs, we have thoroughly revised the manuscript. All the comments and suggestions have been addressed and implemented in this revised manuscript.

Responses to the individual comments can be found below. Unless otherwise specified, the references, equations, figures and tables cited in the answers are numbered as per the revised manuscript.

```
>> REVIEWER 1<<
This paper proposes a new model for estimating the solar irradiance using pictures. This
    method has some new ideas. In particular, this method may play an important role in
    the prediction of solar radiation. But, It seems to me that this research shows a
    kind of preliminary results, so more details and data are required to extract robust
    conclusions. Therefore, this version of the manuscript is not ready for a regular
    article.
```

Thanks for the comment. The core idea of this manuscript is to establish the fact that images obtained from ground-based sky cameras can assist us in accurately estimating the rapid fluctuations of measured solar irradiance. This is the first step, for a robust and reliable short-term solar forecasting. In this manuscript, we restrict our discussions to mainly solar irradiance estimation, and do not delve into solar irradiance prediction.

We have incorporated several major changes in the current version of the manuscript. Some of the major changes include:

- We have provided a detailed discussion of the calibration techniques – white balancing, geometric calibration and vignetting correction, used in our ground-based sky camera;
- We have provided an extensive evaluation of several other non-linear models (or empirical fits) between solar irradiance and image luminance. Instead of a linear model, we have investigated the use of a higher-order polynomial fit to model the irradiance based on image-based luminance. More discussions of these models are provided in Section 3.3 of the revised manuscript; and
- We have also added useful insights on the use of optical flow techniques to forecast the future sky/cloud image. We provided our initial results on estimating the image forecasts with a lead time of upto 15 minutes. We discussed this in Section 5 of the revised manuscript.

In the revised manuscript, these changes are incorporated throughout the manuscript.

```
General comments.
```

1.The most important problem to be explained is the calibration. Because the parameters of each WSIs are different, the new WSIs must be calibrated for six months to one year to achieve solar radiation estimation. This is very limited in practical application. Even so, what is the uncertainty of estimation result?

Thanks for the comment. We agree that the calibration of the ground-based cameras is an important step. Our ground-based camera WAHRSIS is calibrated with respect to – white balancing, geometric calibration and vignetting correction.

The imaging system in WAHRSIS is modified so that it captures the near-infrared region of the spectrum. Hence, the red channel of the captured image is more prone to saturation. It renders the captured image reddish in nature. Therefore, we employ custom white balancing in the camera, such that it compensates the alteration owing to the near-infrared capture. Figure 1 depicts the captured images obtained from automatic and custom white balancing.

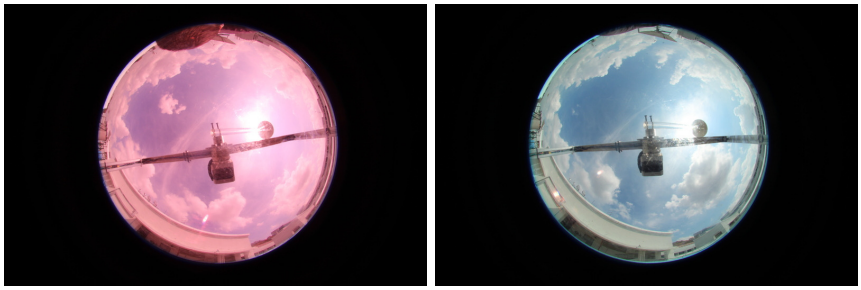

(a) With auto white-balancing (b) With custom white-balancing

Figure 1: We use custom white-balancing for correcting the white balance.

We use the popular toolbox by Scaramuzza *et al.* [1] for the geometric calibration of WAHRSIS. This process involves the computation of the intrinsic parameters of the camera. We use a black-and-white regular checkerboard pattern, and position it at various positions around the sky camera. Figure 2 illustrates a few sample positions of the checkerboard. Using user interaction to identify the corner points and the known 3D co-ordinates, we estimate the intrinsic parameters of the camera.

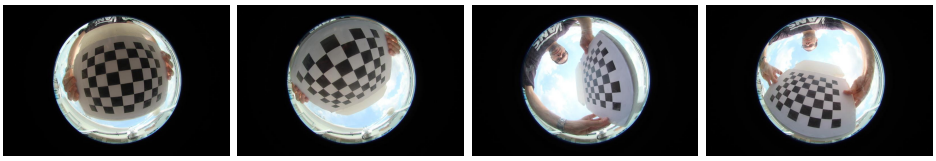

Figure 2: We position the checkerboard at various locations for the geometric calibration.

Finally, we also employ vignetting correction to the images captured by our sky camera. Owing to the fish-eye nature of the lens, the area around the centre of the lens is brighter, as compared to the sides. We use an integrating sphere to correct this variation of illumination. Figure 3 depicts an image captured inside an integrating sphere that provides an uniform illumination distribution in all directions. We use this reference image to correct the illumination of all captured sky/cloud images by our sky camera.

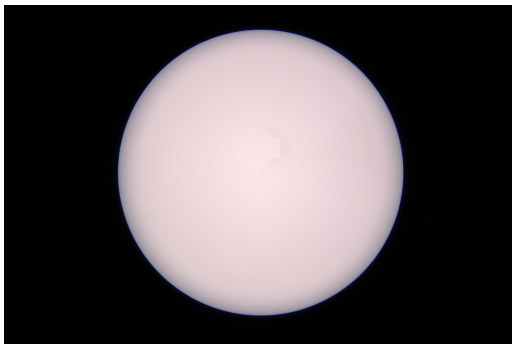

Figure 3: We captured a reference image inside the uniformly-illuminated integrating sphere.

Of course, these calibration techniques are fundamental, and needs to be completed for subsequent analytics using sky cameras. In the revised manuscript, we have mentioned that a prior calibration of the imaging systems is required for estimating solar irradiance from sky cameras.

In the revised manuscript, we have added this discussion in Section 2.1 of the manuscript.

2.The method of determining the sampling points around the sun proposed in this paper is not the core issue in my opinion. In fact, with the sun as the center, the result of determining the sampling point by any method based on distance weighting will not be very different from the result in this paper. Or, the results of these methods should be compared in the paper.

Thanks for the comment in investigating an alternate strategy of sampling. In our previous work [2], we used a cropped version of the image with the sun as the centre. However, we realised that there are several disadvantages to this approach.

- We need to find the position of the sun in the image, in order to crop a square image with the sun as centre. However, this identification becomes difficult during overcast, wherein the sun is completely covered by clouds;
- We also need to ascertain the optimal crop size dimension to obtain the best accuracy. We compute the correlation value between solar irradiance value and image luminance value for various crop size dimensions. Figure 4 shows the impact of crop size on the obtained correlation.

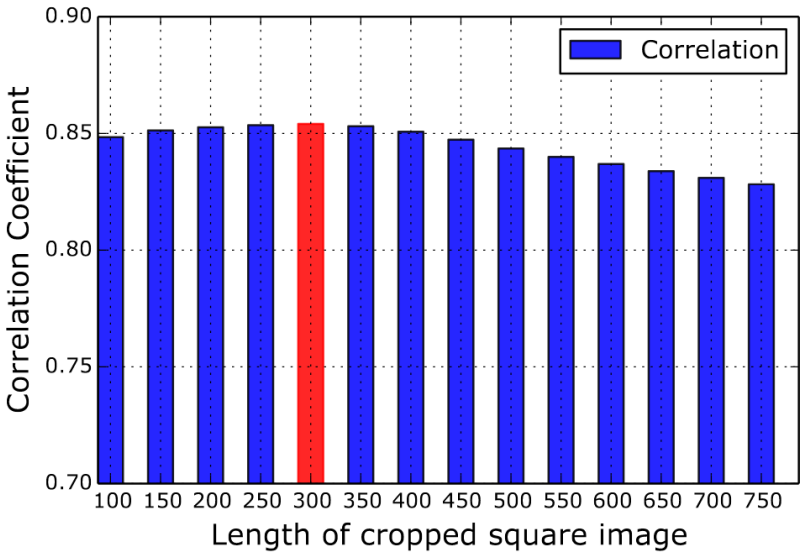

Figure 4: We observe that the best performance is obtained for a crop size of 300×300 (red bar).

Therefore, in order to avoid these demerits, we sample the pixels around the hemispherical dome to estimate the solar irradiance values. Our obtained results (cf. Section 4) establish that such sampling strategy work well in estimating solar irradiance.

In the revised manuscript, we have added this discussion in Section 3.1 of the manuscript.

```
3.Based on the current research, the paper hopes to further realize the prediction of
    solar radiation based on pictures obtained by WSIs. That's really a good idea.
    However, the predicted results should also be given in the article. Because if there
    is no next step to predict radiation, this paper has no practical application value.
    (Solar pyranometers are cheaper and more accurate than WSIs)
```

Thanks for the feedback. We absolutely agree that the full potential of using ground-based sky cameras will be realised in the solar energy *prediction* stage, in addition to the current solar irradiance *estimation*. The main focus of this manuscript is to establish to our community that ground-based imaging systems can provide us useful insights in understanding and estimating the rapid fluctuations of solar irradiance over the different hours of the day. In this paper, we restricted our message to convey this key idea of solar irradiance estimation, and did not delve into solar irradiance forecasting.

However, in this response letter, we provide our initial result on solar irradiance forecasting. We borrow techniques from time series modelling, to forecast future solar irradiance values. In our recent work [3], we modelled the solar irradiance values using triple exponential smoothing (TES). Figure 5 illustrates the performance of TES model for a short lead time. These solar irradiance recordings are measured in the interval of 1 minute. We use a historical data of 1000 observations, to estimate the next 50 observations. We set the seasonal period in TES model as 288. We observe that the predicted solar irradiance values (represented in green color) closely follows the actual solar irradiance values.

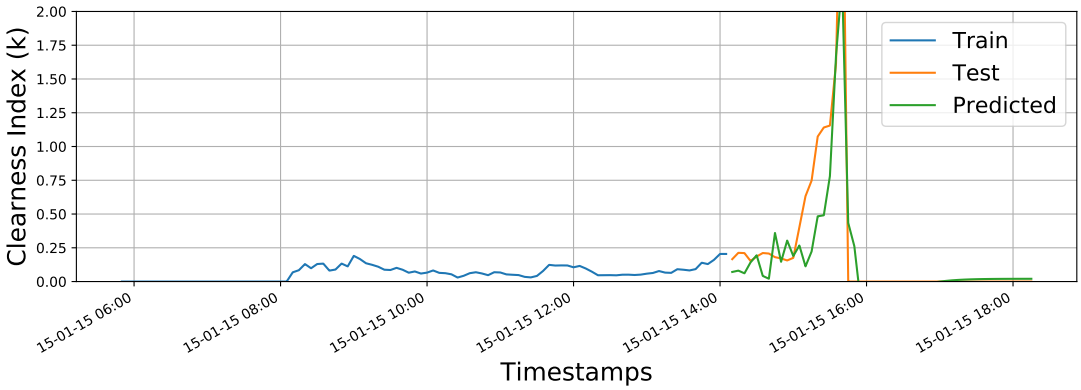

Figure 5: We illustrate the clearness index (k) values in the time series. This clearness index is defined as the ratio of observed solar irradiance and measured solar irradiance. We observe that the predicted solar irradiance values closely matches the actual solar irradiance.

In our upcoming work, we are currently incorporating the TES modelling technique directly on the sky camera image, instead of applying onto solar irradiance point measurements. We hope this will provide a better solar estimation technique than the current state-of-the-art methodologies.

In the revised manuscript, we have added this discussion in Section 6 of the manuscript.

4.The author should pay attention to the prediction of solar radiation, Especially in the first step, cloud motion prediction. There are many problems in cloud motion prediction based on distorted images. How accurate the radiation prediction can be obtained from the predicted image should be explained together.

Thanks for the feedback. We agree that the prediction of cloud motion vectors [4] is the first step in the realm of solar radiation forecasting. We have exploited optical flow techniques to estimate the direction and flow of cloud motion vectors between two successive image frames. We use the $(B - R)/(B + R)$ ratio channel of the sky/cloud image, where B and R are the blue and red channels respectively. We use an implementation [1] of optical flow technique that uses a simpler conjugate gradient solver to obtain the flow field. Figure 6 illustrates the estimated flow field.

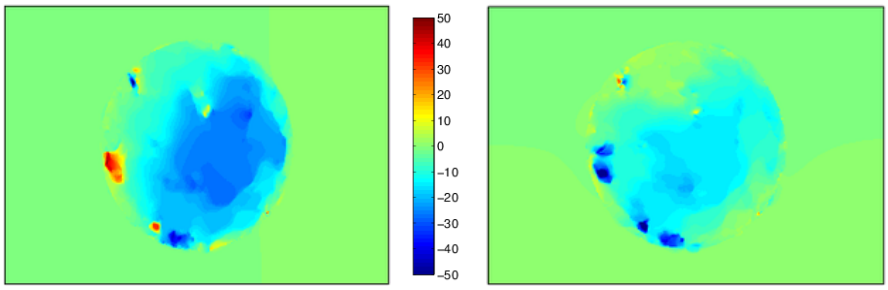

(a) Horizontal translation (b) Vertical translation

Figure 6: We visualize the horizontal and vertical translation of pixels between two successive frames, using optical flow technique.

Using the images captured at t and $t - 2$ minutes, we estimate the horizontal and vertical translation of the pixels. Under the assumption that the flow of cloud motion vectors for the successive $t + 2$ minutes is similar to that of previous frames, we estimate the future $t + 2$ minutes frame, and subsequently the $t + 4$ minutes frame. Figure 7 illustrates this. We obtain a forecast

[1] Available at `https://people.csail.mit.edu/celiu/OpticalFlow/`

accuracy of 70% for a prediction lead time upto 6 minutes. However, the accuracy decreases for a longer lead time. In our future work, we will estimate the solar irradiance value on the predicted sky/cloud image, using the empirical model proposed in this manuscript.

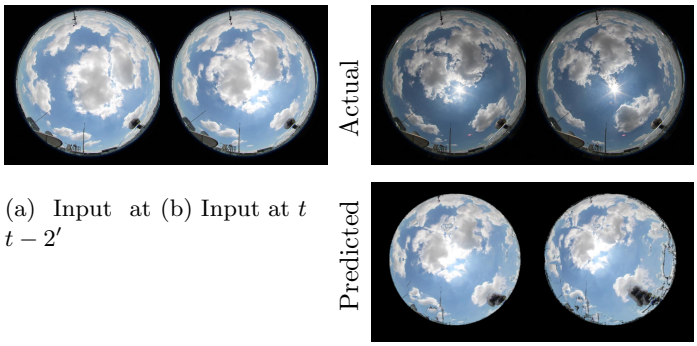

(a) Input at $t - 2'$ (b) Input at t (c) $t + 2'$ (d) $t + 4'$

Figure 7: Prediction of sky/cloud image using optical flow technique.

In the revised manuscript, this discussion is added to Section 5.1 of the manuscript.

`Specific comments`
`5.The references cited in this paper are incorrect.`

Thank you for pointing out. In the revised manuscript, we have ensured that all the references are cited in the AMT style.

In the revised manuscript, these changes are incorporated throughout the manuscript.

`6.Some abbreviations need to be given in full English and even explained. For example, DSLR (P3L29);`

Thanks for the comment. In the revised manuscript, we have provided the full form of digital single-lens reflex (DSLR). We have also provided detailed explanations of DSLR camera.

In the revised manuscript, we have provided the changes in Section 2.1 of the manuscript.

`7.P4L4: Davis Instruments 7440 Weather Vantage Pro, References or detailed explanations are required.`

Thanks for the feedback. We have now added more discussion in the revised manuscript. The solar pyranometer is included in *Davis Instruments 7440 Weather Vantage Pro* weather station. It measures the total solar irradiance flux density in Watt/m^2. On a clear day with no occluding clouds, the solar sensor ideally follows a typical cosine response. Figure 8 shows the theoretical response of the solar sensor in the pyranometer, for varying degrees of solar incident angle.

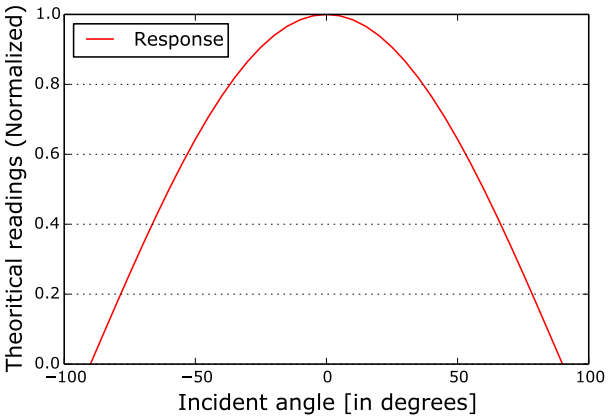

Figure 8: Response of the solar sensor with varying solar incident angle.

In the revised manuscript, the changes are made in Section 2.2 of the manuscript.

`8.How did the P6L9 formula come into being? Is it suitable for use here? Explanation is needed`

Thanks for the comment. The P6L9 formula is used to compute the luminance of an image from the R, G and B values of the RGB image. The formula is proposed in SMPTE Recommended Practice 177 [5].

In the revised manuscript, we added this discussion in Section 3.2 of the manuscript.

`9.P12, Figure 7. Watt/ m2 should be Watt / m2`

Thanks for pointing it out. The superscript in the y-label of the corresponding figure is now depicted properly.

In the revised manuscript, this update is performed in Section 4.2 of the manuscript.

References

[1] D. Scaramuzza, A. Martinelli, and R. Siegwart, "A toolbox for easily calibrating omnidirectional cameras," in *Proc. IEEE/RSJ International Conference on Intelligent Robots and Systems*. IEEE, 2006, pp. 5695–5701.

[2] S. Dev, F. M. Savoy, Y. H. Lee, and S. Winkler, "Estimation of solar irradiance using ground-based whole sky imagers," in *Proc. IEEE International Geoscience and Remote Sensing Symposium (IGARSS)*. IEEE, 2016, pp. 7236–7239.

[3] S. Dev, T. AlSkaif, M. Hossari, R. Godina, A. Louwen, and W. van Sark, "Solar irradiance forecasting using triple exponential smoothing," in *Proc. International Conference on Smart Energy Systems and Technologies (SEST)*. IEEE, 2018, pp. 1–6.

[4] S. Dev, F. M. Savoy, Y. H. Lee, and S. Winkler, "Short-term prediction of localized cloud motion using ground-based sky imagers," in *Proc. IEEE Region 10 Conference (TENCON)*. IEEE, 2016, pp. 2563–2566.

[5] RP SMPTE, "RP 177-1993," *Derivation of Basic Television Color Equations*, 1993.

Response to Reviewers' Comments amt-2019-141: Estimating Solar Irradiance Using Sky Imagers

Soumyabrata Dev, Florian M. Savoy, Yee Hui Lee, Stefan Winkler

August 10, 2019

We would like to thank the Associate Editor and the anonymous reviewers for your valuable comments and suggestions. Based on your inputs, we have thoroughly revised the manuscript. All the comments and suggestions have been addressed and implemented in this revised manuscript.

Responses to the individual comments can be found below. Unless otherwise specified, the references, equations, figures and tables cited in the answers are numbered as per the revised manuscript.

```
>> REVIEWER 2<<
This paper presents a method to quantify the solar irradiance by using an all-sky imager
    with a fish eye lens. This uses data sampled in Singapore, with variations in cloudy
    scenes, and is aimed at better prediction of photovoltaic energy production. This
    paper describes a model by which a sky images individual pixels, from compressed jpg,
    are used to related to a
```

Thanks for your positive feedback to this manuscript. We believe that an accurate estimation of the solar irradiance using the ground-based cameras is the first step for a reliable short-term solar forecasting.

```
The paper is mostly well written, and concise, bordering on too short.
```

Thanks for your positive feedback on the writing style of the manuscript. In this manuscript, we kept our message clear and concise on the use of sky cameras for solar irradiance estimation.

In the revised manuscript, we have added more extensive details and explanations. Some of the major changes include:

- We have provided a detailed discussion of the calibration techniques – white balancing, geometric calibration and vignetting correction, used in our ground-based sky camera;
- We have provided an extensive evaluation of several other non-linear models (or empirical fits) between solar irradiance and image luminance. Instead of a linear model, we have investigated the use of a higher-order polynomial fit to model the irradiance based on image-based luminance. More discussions of these models are provided in Section 3.3 of the revised manuscript; and
- We have also added useful insights on the use of optical flow techniques to forecast the future sky/cloud image. We provided our initial results on estimating the image forecasts with a lead time of upto 15 minutes. We discussed this in Section 5 of the revised manuscript.

In the revised manuscript, these changes are incorporated throughout the manuscript.

```
The approach is interesting, and the applications may be wide ranging for energy
    forecasting. That said, the model is not well described, with major issues concerning
     the non-linearity and the normalization factor, that seems to make the model results
     look better than actuality. Model here is also a bit of a stretch as it is simply an
     empirical fit of the measured values.
```

Thanks for the comment.

The main idea of this manuscript is to establish that images obtained from sky camera can be used to estimate the rapid fluctuations of solar irradiance observed throughout the day. The theoretical clear sky model follows a cosine response. In order to map the computed image luminance to follow the similar cosine clear sky model, we use the normalization factor.

In the revised manuscript, we have provided more details about our proposed methodology. As suggested by you, we renamed *model* to *empirical fit*, in order to better convey our proposed message. In the revised manuscript, we provided other non-linear empirical fits between image luminance and solar irradiance. Figure 1 describes the various linear and non-linear fits, using our proposed methodology. We observe that the higher-order polynomials (quartic and quintic) are highly ill-conditioned.

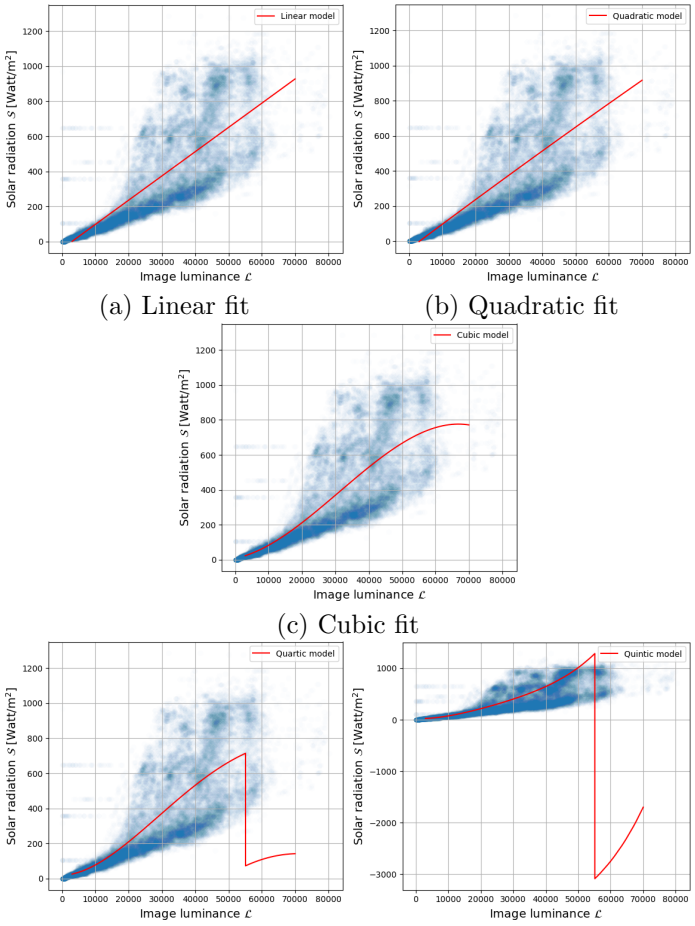

(a) Linear fit (b) Quadratic fit

(c) Cubic fit

(d) Quartic fit (e) Quintic fit

Figure 1: Empirical fit between solar radiation and image luminance computed with our proposed framework. We observe that it deviates from linearity at higher luminance values. Also, the higher order polynomials are ill-conditioned.

We also compute the Root Mean Square Error (RMSE) value between the actual- and regressed-values. Table 1 summarises the performance of the different order polynomials.

Proposed models	**RMSE** (Watt/m^2)
Linear model (degree 1)	178.27
Quadratic model (degree 2)	178.26
Cubic model (degree 3)	176.57
Quartic model (degree 4)	176.52
Quintic model (degree 5)	176.49

Table 1: Performance evaluation of various polynomial order regressors. We measure the RMSE value for each of the models.

We observe that lower order polynomials of degree 1 and 2 perform slightly inferior to those of higher order polynomials. We observe that the performance of cubic, quartic and quintic models are similar. We observe that the quartic and quintic models are highly ill-conditioned from Fig. 1. The cubic model is the best fit, therefore we propose this in our revised manuscript.

In the revised manuscript, these changes are incorporated in Section 3.3 of the manuscript.

`The actual evaluation of the model requires a normalization factor based on the difference to what is considered truth, the irradiance pyranometer measurements.`

Thanks for the feedback. During the evaluation stage, the estimated solar irradiance value is, in fact, compared with the actual irradiance values obtained from the solar sensors. This may not be very clear in the earlier version of the paper. We have re-emphasized the same in the revised manuscript.

In the revised manuscript, we have added this discussion in Section 4.1 of the manuscript.

`There are some instances of colloquial use of English language, while most of the citations are not well formatted. The large use of footnotes also seems to be distracting to the content.`

Thanks for this important feedback. We have revised the sentences in the revised manuscript, and also ensured that all citations are formatted in the AMT style. We have also reduced the number of usage of the citations throughout the paper.

In the revised manuscript, these changes are incorporated throughout the paper.

`The benchmarking technique against other models seems to be lacking most of the state-of-the-art techniques that can easily be found through literature review. Techniques described by Chu et al., 2015, Baharin et al., 2016 for all sky imagers, or satellite -based methods such as the start from Mueller et al., 2004. There are likely many more methods, but just to name a few not reference in this manuscript. Because of the questions on the model assumptions, and its evaluation against dated models, this manuscript does not seem to meet the criteria for publication unless there is significant rework.`

Thanks for your suggestions on the related work. We have added discussion of these publications in Section 1.1 of the revised manuscript. Baharin *et al.* proposed a machine-learning forecast model for PV power output, using Malaysia as the case study. Similarly Chu *et al.* used a reforecasting method to improve the PV power output forecasts with a lead time of 5, 10, and 15 minutes. Mueller *et al.* proposed a clear sky model that is based on radiative transfer models obtained from Meteosat's atmospheric parameters.

The focus of our manuscript is to estimate the solar irradiance values, from ground-based observations. We do not discuss about solar forecasts in this paper. Therefore, we have benchmarked with only those methods that attempt to estimate solar irradiance from ground-based observations. Both Baharin *et al.* and Chu *et al.* discuss solar forecast methodologies, and Mueller *et al.* discuss about satellite-based clear sky modelling.

`The simplistic approach does seem to have merit, but it may be over stated.`

Thanks for the comment. We indeed kept a simple approach to map the solar irradiance to the image-based luminance. Our idea is to establish that that ground-based sky cameras can provide

us more information about the evolution of clouds, as compared to point-based solar pyranometers. The luminance computed from sky camera images can match the rapid fluctuations of the measured solar irradiance.

General Comments:

1. The abstract details 'accurate' but a root mean square deviation of 178 W/m^2 is hardly accurate. The other state of the art methods should be described or at least mentioned.

Thanks for the feedback. As suggested, we have edited the abstract of the revised manuscript in indicating the performance of the proposed methodology. We have also added the benchmarking methods in the abstract.

In the revised manuscript, these changes are indicated in the abstract of the manuscript.

2. Throughout the manuscript, the citations are not in the AMT style. They are often mostly added to end of sentences without proper brackets.

Thanks for pointing it out. In the revised manuscript, we have ensured that citations are referenced in the AMT style.

In the revised manuscript, these changes are incorporated in all sections of the paper.

3. The use of random points in the modelling of the solar irradiance is not well described. Why not use the entire image, and subsetting by using a cloud mask?

Thanks for the feedback. In our previous work [1], we used a cloud mask around the sun to estimate the solar irradiance. However, there are several disadvantages to the cloud mask approach:

- We need to find the position of the sun in the image, in order to crop a square image with the sun as centre. However, this identification of the sun in the image becomes difficult during overcast condition, wherein the sun is completely covered by clouds;
- We also need to ascertain the optimal crop size dimension to obtain the best accuracy. We compute the correlation value between solar irradiance value and image luminance value for various crop size dimensions. Figure 2 shows the impact of crop size on the obtained correlation.

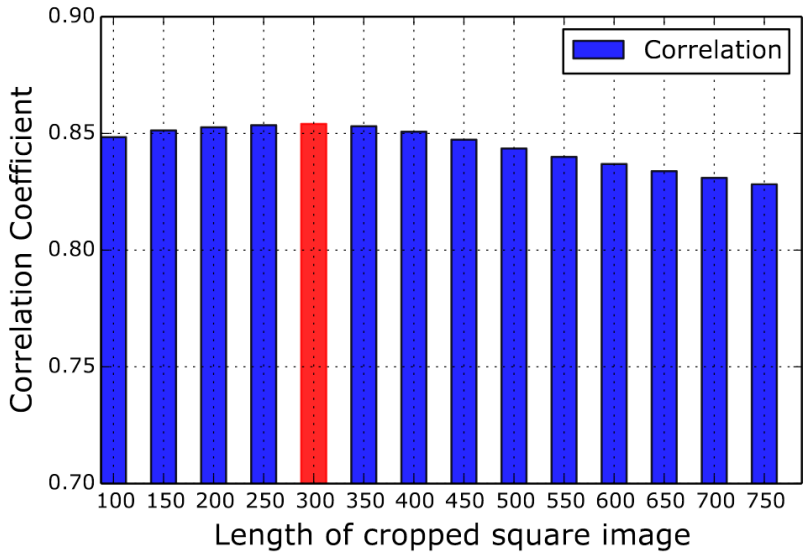

Figure 2: We observe that the best performance is obtained for a crop size of 300×300 (red bar).

Therefore, in order to avoid these demerits, we sample the pixels around the hemispherical dome to estimate the solar irradiance values. Our obtained results (cf. Section 4) establish that such sampling strategy work well in estimating solar irradiance.

In the revised manuscript, we have added this discussion of alternative strategies in Section 3.1 of the manuscript.

4. The irradiance definition is not commonplace for atmospheric research: "The first step in estimating irradiance from the luminance is thus to cosine weight it according to its direction of flow" (p. 7 line 22-23). It should be cosine weighted per regards to the normal of a horizontal plane.

Thanks for the comment. Based on empirical evidences, we use a cosine weight according to the direction of flow. This provided us the best results as compared to other strategies, and hence we proceeded with the same.

In the revised manuscript, we have added this discussion in Section 3.3 of the manuscript.

5. Footnotes should be either incorporated directly into the text, or as citations. Many caveats and omissions are found in the footnotes that should be more explicitly presented.

Thanks for the feedback. In the revised manuscript, we have ensured to use the minimum number of footnotes. Most of the citations are removed, and included directly onto the text.

In the revised manuscript, these changes are incorporated throughout the manuscript.

6. Since much of the manuscript relies on comparing to pyranometer measurements, a more in-depth description of such instrument should be included.

Thanks for the feedback. We have now added more discussion of the solar pyranometer in the revised manuscript. The solar pyranometer is included in *Davis Instruments 7440 Weather Vantage Pro* weather station. It measures the total solar irradiance flux density in Watt/m^2. On a clear day with no occluding clouds, the solar sensor ideally follows a typical cosine response. Figure 3 shows the theoretical response of the solar sensor in the pyranometer, for varying degrees of solar incident angle.

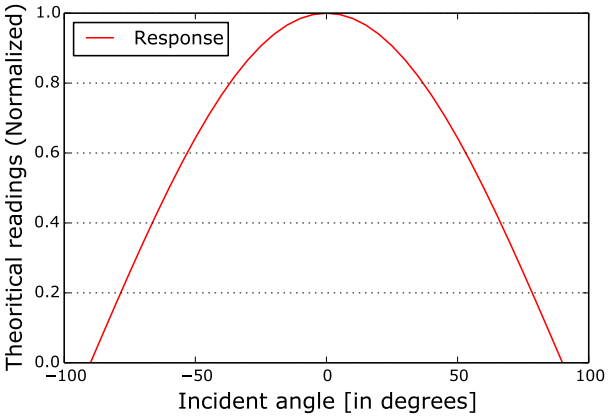

Figure 3: Response of the solar sensor with varying solar incident angle.

In the revised manuscript, the changes are made in Section 2.2 of the manuscript.

7. The discussion of the non-linearity seems to be rather lacking of analytical analysis.

Thanks for the comment. We use *JPEG* images instead of uncompressed *RAW* images for the computation of scene luminance. The *JPEG* compression algorithm introduces non-linearities in the pixel values and, therefore our proposed empirical fit deviates from a linear relationship. We

can generate more consistent results by using only *RAW* format images. In our future work, we intend to use *RAW* format images for the computation of solar irradiance values from sky cameras.

In the revised manuscript, we have included this discussion in Section 5 of the manuscript.

8. The normalization factor depends on having both irradiance and all sky imaging - this seems to be hiding the discrepancies of the model. Leaves the reader doubting the results from figure 4 and 5.

Thanks for the comment on the normalization factor. The theoretical clear sky model follows a cosine response. In order to map the computed image luminance to follow the similar cosine clear sky model, we use the normalization factor. The main idea in this manuscript is to establish an empirical model of the image luminance, that can estimate the rapid fluctuations of the solar irradiance.

In the revised manuscript, we have added this discussion in Section 4.1 of the manuscript.

Specific Comments:

9. P.2 lines 3 13, missing multiple citations for MODIS products, GEOSS, Ouarda et al. citation is oddly written. SEVIRI acronym not defined.

Thanks for the feedback. We have added references for MODIS [2] and GEOSS [3]. The Ouarda *et al.* citation is now fixed. We have also spelled out SEVIRI as Spinning Enhanced Visible and Infrared Imager.

In the revised manuscript, the changes are incorporated in Section 1 of the manuscript.

10. P.2 line 23, What are "hot belts" ? This regional language use should be amended for a more understood English sentence.

Thanks for the feedback. Our intended meaning is that tropical countries are more conducive for solar energy generation, because of the large amount of incident sunlight throughout the year. We have removed the phrase 'hot belts', and rephrased the sentence for no confusion.

In the revised manuscript, the changes are incorporated in Section 1.1 of the manuscript.

11. P.6, footnote could be inserted into text, also there is no reference to "SMPTE recommended Partice 177"

Thanks for the feedback. We have removed the corresponding footnote, and included it inline with the text. We have also added reference to the SMPTE Recommended Practice 177 [4] to the revised manuscript.

In the revised manuscript, the changes are incorporated in Section 3.2 of the manuscript.

12. P. 7, footnote should be a full citation and inserted within text.

Thanks for the feedback. The footnote in pp. 7 is now removed, and inserted within the text. In the revised manuscript, we have ensured to use the minimum number of footnotes. They are now mostly inserted within the texts, or omitted.

In the revised manuscript, the changes are incorporated in 3.3 of the revised manuscript.

References:

Baharin, K. A., Abdul Rahman, H., Hassan, M. Y. and Gan, C. K.: Short-term forecasting of solar photovoltaic output power for tropical climate using ground-based measurement data, J. Renew. Sustain. Energy, 8(5), 53701, doi:10.1063/1.4962412, 2016.

Chu, Yinghao & Urquhart, Bryan & Gohari, S M Iman & Pedro, Hugo & Kleissl, Jan &F.M. Coimbra, Carlos: Short-term reforecasting of power output from a 48 MWe solar PV plant. Solar Energy. 112. 68-77. 10.1016/j.solener.2014.11.017, 2015.

Mueller, R. W., Dagestad, K. F., Ineichen, P., Schroedter-Homscheidt, M., Cros, S., Dumortier, D., Kuhlemann, R., Olseth, J. A., Piernavieja, G., Reise, C., Wald, L. and Heinemann, D.: Rethinking satellite-based solar irradiance modelling: The SOLIS clear-sky module, Remote Sens. Environ., 91(2), 160 174 , doi: https://doi.org/10.1016/j.rse.2004.02.009, 2004.

Thanks for sharing the list of references. We have added discussion of this related methods [5, 6, 7] in Section 1.1 of the manuscript, and included them in the reference list.

In the revised manuscript, these changes are incorporated in Section 1.1 and References Section.

References

[1] S. Dev, F. M. Savoy, Y. H. Lee, and S. Winkler, "Estimation of solar irradiance using ground-based whole sky imagers," in *Proc. IEEE International Geoscience and Remote Sensing Symposium (IGARSS)*. IEEE, 2016, pp. 7236–7239.

[2] T. S. Pagano and R. M. Durham, "Moderate resolution imaging spectroradiometer (MODIS)," in *Proc. Sensor Systems for the Early Earth Observing System Platforms*. International Society for Optics and Photonics, 1993, vol. 1939, pp. 2–17.

[3] C. C. Lautenbacher, "The global earth observation system of systems: Science serving society," *Space Policy*, vol. 22, no. 1, pp. 8–11, 2006.

[4] RP SMPTE, "RP 177-1993," *Derivation of Basic Television Color Equations*, 1993.

[5] K. A. Baharin, H. Abdul Rahman, M. Y. Hassan, and C. K. Gan, "Short-term forecasting of solar photovoltaic output power for tropical climate using ground-based measurement data," *Journal of renewable and sustainable energy*, vol. 8, no. 5, pp. 053701, 2016.

[6] Y. Chu, B. Urquhart, S. MI Gohari, H. TC Pedro, J. Kleissl, and C. FM Coimbra, "Short-term reforecasting of power output from a 48 MWe solar PV plant," *Solar Energy*, vol. 112, pp. 68–77, 2015.

[7] RW Mueller, K-F Dagestad, P. Ineichen, M Schroedter-Homscheidt, S. Cros, D. Dumortier, R. Kuhlemann, JA Olseth, G. Piernavieja, C. Reise, et al., "Rethinking satellite-based solar irradiance modelling: The SOLIS clear-sky module," *Remote sensing of Environment*, vol. 91, no. 2, pp. 160–174, 2004.

Estimating Solar Irradiance Using Sky Imagers

Soumyabrata Dev[1,2], Florian M. Savoy[3], Yee Hui Lee[4], and Stefan Winkler[3,5]

[1]ADAPT SFI Research Centre, Dublin, Ireland
[2]School of Computer Science, University College Dublin, Ireland
[3]Advanced Digital Sciences Center (ADSC), University of Illinois at Urbana-Champaign, Singapore 138632
[4]School of Electrical and Electronic Engineering, Nanyang Technological University (NTU), Singapore 639798
[5]School of Computing, National University of Singapore

Correspondence to: Stefan Winkler (winkler@comp.nus.edu.sg)

Abstract. Ground-based whole sky cameras are now-a-days extensively used for localized monitoring of the clouds. They capture hemispherical images of the sky at regular intervals using a fisheye lens. In this paper, we ~~derive a model~~ propose a framework for estimating the solar irradiance using pictures taken by those imagers. Unlike pyranometers, these sky images contain information about the cloud coverage and can be used to derive cloud movement. An accurate estimation of the solar irradiance using solely those images is thus a first step towards short-term solar energy generation forecasting, as cloud movement can also be derived from them. We derive and validate our model using pyranometers co-located with our whole sky imagers. We achieve a ~~root mean square error of 178 Watt/m^2 between estimated and measured~~ better performance in estimating the solar irradiance, ~~outperforming state-of-the-art methods using other weather instruments~~as compared to other related methods using ground-based observations. Our method shows a significant improvement in estimating strong short-term variations~~.~~, as compared to methods Hargreaves and Samani (Hargreaves and Samani, 1985), Bristow and Campbell (Bristow and Campbell, 1984), Donatelli and Campbell (Donatelli and Campbell, 1998) and Hunt *et al.* (Hunt et al., 1998).

1 Introduction

Clouds have a significant impact on solar energy generation. They intermittently block the sun and significantly reduce the solar irradiance reaching solar panels. A short-term forecast of the solar irradiance is needed for the grid operators to mitigate the effects of a power generation ramp-down. With rapid developments in photogrammetric techniques, ground-based sky cameras are now widely used ~~Dev et al. (2016e)~~(Dev et al., 2016e). These cameras, known as Whole Sky Imagers (WSIs) are upward looking devices that captures the sky scene at regular intervals of time. The images captured by WSIs are subsequently used for automatic cloud coverage computation, cloud tracking and cloud base height estimation. In our research group, we use these imagers to study the effect of clouds in satellite communication links ~~Dev et al. (2018b); Yuan et al. (2016); Dev et al. (2016a)~~(Dev et al., 2018

Localized and short-term forecasting of cloud movements is an on-going research topic ~~Shakya et al. (2017); Jiang et al. (2017); Feng et~~ Optical flow techniques can be used to generate forecasted images using two anterior frames ~~Dev et al. (2016d)~~(Dev et al., 2016d). Similar cloud motion vectors are exploited in satellite images for solar power prediction ~~Jang et al. (2016)~~(Jang et al., 2016).

Our proposed method in estimating solar irradiance is thus a first step towards solar irradiance forecasting, as the input data used to estimate the irradiance is the same as the one used to forecast the sky condition.

The accurate estimation of solar energy is a challenging task, as clouds greatly impact the total irradiance received on the earth's surface. In the event of clouds covering the sun for a short time, there is a sharp decline of the produced solar energy. Therefore, it is of utmost importance to model the incoming solar radiation accurately. In this paper, we answer this fundamental question: can the rapid fluctuations of the solar irradiance be captured? We perform this by using ground-based sky cameras to estimate the solar irradiance.

The analysis of clouds and several other atmospheric phenomenon is traditionally done using satellite images. However, these satellite images have low temporal and spatial resolutions. The most widely used satellite data is from Moderate-resolution Imaging Spectroradiometer (MODIS) (Pagano and Durham, 1993), which is on board the Terra and Aqua satellites. They provide a large-scale view of the cloud dynamics and various atmospheric phenomenons. The data from this satellite on-board instruments are usually available only twice in a day. This is useful for a macro-analysis of cloud formation at a particular location on the earth's surface. One of the illustrative examples of such satellite data is the HelioClim-1 database from Global Earth Observation System of Systems (GEOSS) (Lautenbacher, 2006). It provides hourly and daily average of surface solar radiation received at ground level ~~Lefèvre et al. (2014)~~(Lefèvre et al., 2014). Ouarda et al. in ~~Ouarda et al. (2016)~~ (Ouarda et al., 2016) assessed the solar irradiance from six thermal channels obtained from ~~SEVIRI~~ Spinning Enhanced Visible and Infrared Imager (SEVIRI) instrument. However these information are temporal and spatial averages. Solar energy applications requires knowledge of the solar irradiance at specific locations and at every time throughout the day. Therefore, images obtained from satellite are not conducive for analysis, especially in geographical small countries like Singapore where the cloud formation is highly localized.

1.1 Related Work

Several existing works analyze ground-based images with different meteorological observations. Most of them correlate the cloud coverage obtained from the sky images with the human observations from meteorological centers. Silva and Souza-Echer validated cloud coverage measurements obtained from ground-based automatic imager and human observations for two meteorological stations in Brazil ~~Silva and Souza-Echer (2016)~~(Silva and Souza-Echer, 2016). Huo and Lu also performed such field experiments for three sites in China ~~Huo and Lu (2012)~~(Huo and Lu, 2012). The computation of such cloud coverage percentage is important in solar energy generation. It can hugely impact the amount of solar radiation falling at a particular place. The correct estimation of solar irradiance, is particularly important in tropical countries like Singapore, where the amount of received solar irradiance is high. Rizwan et al. in ~~Rizwan et al. (2012)~~ (Rizwan et al., 2012) have demonstrated that tropical countries are ~~hot belts~~ conducive for installing large central power stations ~~,~~ powered by solar energy, because of the large amount of incident sunlight throughout the year. Several attempts have been done to estimate the solar radiation from general meteorological measurements via temperature, humidity and precipitation ~~Hargreaves and Samani (1985); Donatelli and Campbell (1998);~~ These existing models aim to provide global solar radiation using different sensors. Alsadi and Nassar in ~~Alsadi and Nassar (2017)~~ (Alsadi a demonstrated such estimation models from the perspective of a photovoltaic solar field. They have effectively demonstrated that the succeeding rows in a photovoltaic solar field receive less solar radiation than that of first row. They also provided an analyti-

cal solution by including the design parameters in the estimation model. In addition to solar irradiance estimate, there have been several efforts in forecasting the solar irradiance with a lead time of few minutes. Baharin *et al.* proposed a machine-learning forecast model for PV power output, using Malaysia as the case study (Baharin et al., 2016). Similarly Chu *et al.* used a reforecasting method to improve the PV power output forecasts with a lead time of 5, 10, and 15 minutes (Chu et al., 2015). Satellite images have also been used in the realm of solar analytics. Mueller *et al.* proposed a clear sky model that is based on radiative transfer models obtained from Meteosat's atmospheric parameters (Mueller et al., 2004). However, satellite data have lower temporal and spatial resolutions. Recently, with the development of low-cost photogrammetric techniques, sky camera are being deployed for such purposes. These sky cameras have a higher temporal and spatial resolutions, and provide a more localized information about the atmospheric events. Alonso-Montesinos and Batlles used sky cameras to quantify the total solar radiation ~~Alonso-Montesinos and Batlles (2015)~~(Alonso-Montesinos and Batlles, 2015). Yang and Chen studied these solar irradiance variability using entropy and covariance ~~Yang and Chen (2015)~~(Yang and Chen, 2015). Dev et al. in ~~Dev et al. (2018a)~~ (Dev et al., 2018a) used triple exponential smoothing for analyzing the seasonality of the solar irradiance. However, these approaches could not model the sharp short-term variations of solar radiation.

1.2 Outline of our work

In this paper, we use images obtained from WSIs to accurately model the fluctuations of the solar radiation. There are several advantages of using a WSI to estimate solar irradiance, instead of using a pyranometer. Common weather stations generally uses a solar sensor that measures the total solar irradiance. It is a point-source device providing information for a particular location. It does not provide information on cloud macrophysical properties, and its evolution over time. On the other hand, the wide-angle view of ground-based sky camera provide us extensive information of the sky. It allows for the tracking of cloud mass over successive image frames, and also predict its future location. In this paper, we attempt to solve the fundamental problem of modeling solar irradiance from sky images. This will also help in solar energy forecasting, which is useful in photovoltaic (PV) systems ~~Lorenz et al. (2009)~~(Lorenz et al., 2009).

~~In our previous work Dev et al. (2016b), we analyzed the region around the sun (known as circumsolar region) and illustrated the effect of clouds around the sun on the direct solar irradiance.~~

The main contributions of this paper ~~compared to our earlier work include~~are as follows:

- A robust framework to accurately estimate and track the rapid fluctuations of solar irradiance;
- A proposal of ~~a solar irradiance model~~ estimating solar irradiance using ground-based sky camera images;
- An extensive benchmarking of our proposed ~~model~~ method with other solar irradiance estimation models.

The rest of the paper is organized as follows. Section 2 describes our experimental setup that captures the sky/cloud images and collects other meteorological sensor data. Our framework for estimating solar irradiance ~~along with the proposed model~~ is detailed in Section 3. Section 4 discusses the evaluation of our ~~proposed model~~approach, and its benchmarking with other existing solar estimation models. We discuss the possible applications of our approach in Section 5. We also point out a few limitations of our approach, and ways to address them. Section 6 concludes the paper.

2 Data Collection

Our experimental setup consists of weather stations and ground-based WSIs. These devices are collocated at the rooftop of our university building (1.34°N, 103.68°E). These devices continuously capture the various meteorological data, and archive them for subsequent analysis.

2.1 Whole Sky Imager (WSI)

Commercial WSIs are available in the market. However, those imagers have high cost, low image resolution, and less flexibility in operation. In our research group, we have designed our custom-built, low-cost, and high-resolution sky imagers. These imagers are called WAHRSIS, that stands for Wide Angle High Resolution Sky Imaging System ~~Dev et al. (2014)~~(Dev et al., 2014). A WAHRSIS imager essentially consists of a high-resolution ~~*DSLR*~~ digital single-lens reflex (DSLR) camera with a fish-eye lens and an on-board micro-computer. The DSLR camera has a digital imaging sensor, instead of the traditional photographic film. The entire device is sealed inside a box with a transparent dome for the camera. Over the years, we have built several versions of WAHRSIS ~~Dev et al. (2014, 2015)~~(Dev et al., 2014, 2015). They are now deployed at several rooftops of our university campus, capturing images of the sky at intervals of 2 minutes.

Our ground-based camera WAHRSIS is calibrated with respect to – white balancing, geometric calibration and vignetting correction. The imaging system in WAHRSIS is modified so that it captures the near-infrared region of the spectrum. Hence, the red channel of the captured image is more prone to saturation. It renders the captured image reddish in nature. Therefore, we employ custom white balancing in the camera, such that it compensates the alteration owing to the near-infrared capture. Figure 1 depicts the captured images obtained from automatic and custom white balancing.

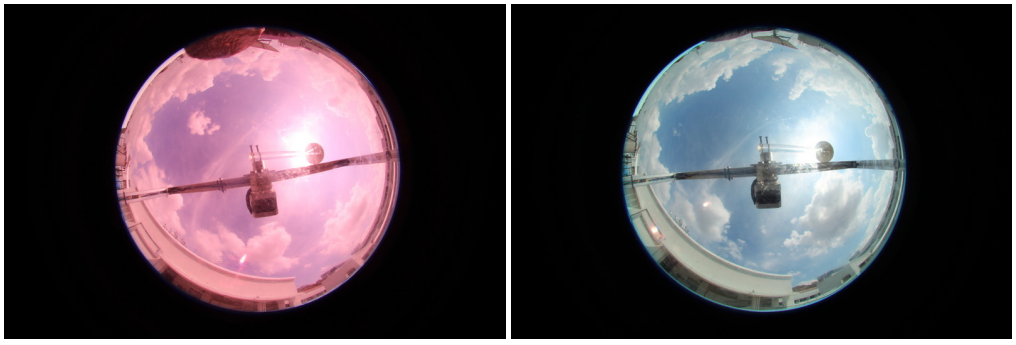

(a) With auto white-balancing (b) With custom white-balancing

Figure 1. We use custom white-balancing for correcting the white balance.

We use the popular toolbox by Scaramuzza *et al.* (Scaramuzza et al., 2006) for the geometric calibration of WAHRSIS. This process involves the computation of the intrinsic parameters of the camera. We use a black-and-white regular checkerboard pattern, and position it at various positions around the sky camera. Figure 2 illustrates a few sample positions of the checkerboard.

Using user interaction to identify the corner points and the known 3D co-ordinates, we estimate the intrinsic parameters of the camera.

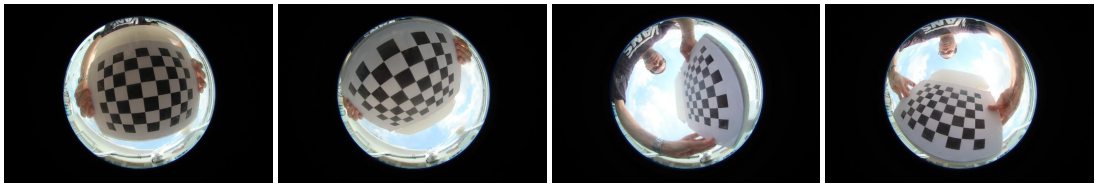

Figure 2. We position the checkerboard at various locations for the geometric calibration.

Finally, we also employ vignetting correction to the images captured by our sky camera. Owing to the fish-eye nature of the lens, the area around the centre of the lens is brighter, as compared to the sides. We use an integrating sphere to correct this variation of illumination. Figure 3 depicts an image captured inside an integrating sphere that provides an uniform illumination distribution in all directions. We use this reference image to correct the illumination of all captured sky/cloud images by our sky camera.

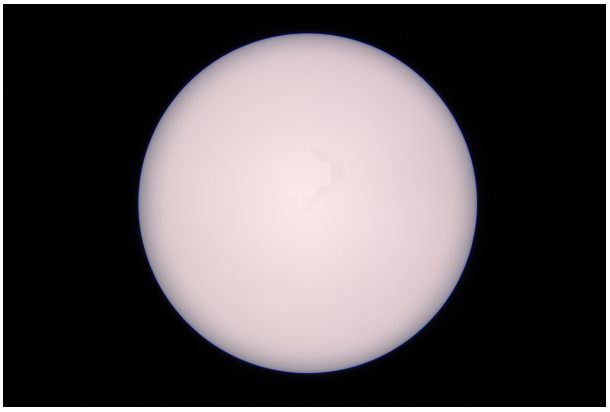

Figure 3. We captured a reference image inside the uniformly-illuminated integrating sphere.

2.2 Weather Station

In addition to the sky imagers, we have also installed collocated weather stations. We use *Davis Instruments 7440 Weather Vantage Pro* for our recordings. It measures rainfall, total solar radiation, temperature and pressure at intervals of 1 minute. The resolution of the tipping-bucket rain gauge is 0.2 mm/tip.

It also includes a solar pyranometer measuring the total solar irradiance flux density in Watt/m^2. This consists of both direct and diffused solar irradiance component. The solar sensor integrates the solar irradiance across all angles, and provide the net

solar irradiance. On a clear day with no occluding clouds, the solar sensor ideally follows a typical cosine response. Figure 4 shows the theoretical response of the solar sensor in the pyranometer, for varying degrees of solar incident angle. The solar sensor reading is highest during noon when the incident angle of sun rays is at the minimum, whilst the reading is low during morning and evening hours.

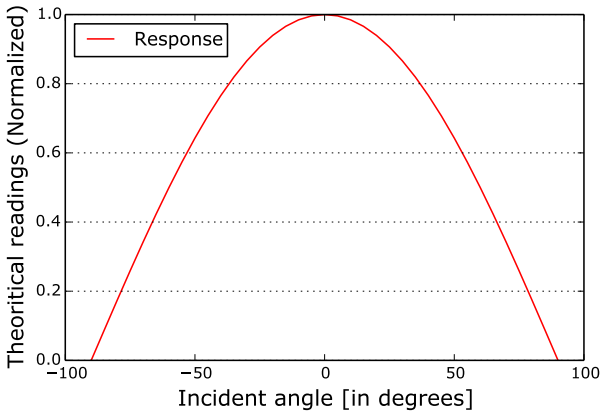

Figure 4. Response of the solar sensor with varying solar incident angle.

The solar radiation on a clear sky can be modeled using the solar zenith angle, and earth's eccentricity. Several clear sky models have been developed for various regions. The best clear-sky model for Singapore is provided by Yang ~~et al. Yang et al. (2012).~~ *et al.* (Yang et al., 2012). We performed a comparison of various clear sky models in Singapore ~~Dev et al. (2017)~~(Dev et a and found that the Yang ~~et al.~~ *et al.* provides a good estimate of the clear sky irradiance. The clear-sky Global Horizontal Irradiance (GHI) G_c is modeled as:

$$G_c = 0.8277 E_0 I_{sc} (\cos\alpha)^{1.3644} e^{-0.0013\times(90-\alpha)}, \quad (1)$$

where E_0 is the eccentricity correction factor for earth, I_{sc} is the solar irradiance constant (1366.1Watt/m^2), and α is the solar zenith angle (measured in degrees). The factor E_0 is calculated as:

$$E_0 = 1.00011 + 0.034221\cos(\Gamma) + 0.001280\sin(\Gamma) + 0.000719\cos(2\Gamma) + 0.000077\sin(2\Gamma),$$

where $\Gamma = 2\pi(d_n - 1)/365$ is the day angle (measured in radians) and d_n is the day number of the year.

As an illustration, we show the clear-sky radiation for the 1st of September 2016 in Fig. 5. The actual solar radiance measured by our weather station is also plotted. We also show the deviation of the measured solar radiation from the clear-sky model. We observe that there are extremely rapid fluctuations in the measured readings. In our previous work ~~Dev et al. (2016b)~~(Dev et al., 2016b),

we observed that these rapid fluctuations caused by the incoming clouds that obstruct the sun from direct view. Such information about the cloud profile and its formation cannot be obtained from a point-source solar recording. Therefore, we aim to model these rapid fluctuations in the measured solar radiation from wide-angle images captured by our sky cameras.

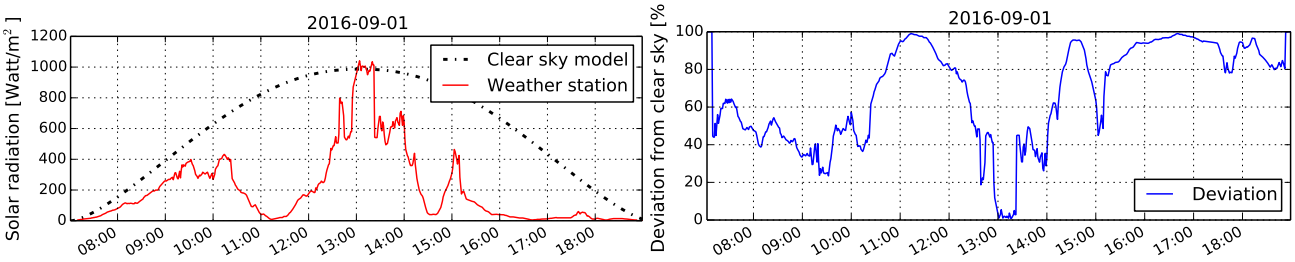

(a) Measured solar radiation along with clear-sky model.

(b) Percentage deviation of solar radiation from clear sky data.

Figure 5. Solar radiation measurements on the 1st of September 2016. Note the rapid fluctuations of high magnitude in the measured solar radiation recording.

3 Modeling Solar Irradiance

This section details our model for computing the solar irradiance from images captured by a whole sky imager. We sample pixels using a cosine weighted hemispheric sampling to simulate the behavior of a pyranometer based on the fisheye camera lens. We then compute the relative luminance using the image capturing parameters, after gamma correction. We finally derive a ~~linear regressor~~ empirical fitting function to scale the computed luminance to match measured irradiance values.

3.1 Cosine weighted hemispheric sampling

The behavior of our fisheye lens with focal length f is modeled by the equisolid equation $r = 2f\sin(\theta/2)$, relating the distance (r) of any pixel from the center of the image to its incident light ray elevation angle (θ). This allows to project a captured image on a unit hemisphere, as shown in Fig. 6a.

The solar irradiance is composed of a direct component relating the sun light reaching the earth without interference, as well as diffuse and reflected components. Given the high resolution of our images, we consider randomly sampled pixel locations on the hemisphere as input to the luminance computation. We follow a cosine weighted hemispheric distribution function, the center of which is at the location of the sun. This is because clouds in the circumsolar region have the highest impact on the total solar irradiance received on the earth's surface ~~Dev et al. (2016b)~~(Dev et al., 2016b). We provide more emphasis to the clouds around the sun, as compared to those near the horizon. In our previous work (Dev et al., 2016c), we used a cloud mask around the sun to estimate the solar irradiance. However, such methods needs an additional task of optimizing the size of the cropped image for best results. Therefore, we adopted this strategy of cosine weighted hemispheric sampling.

The first step is to compute the sampled locations from the top of the unit hemispheric dome. Each of the locations are computed as follows, using two random floating points R_1 and R_2 as input, where $(0 \leq R_1, R_2 \leq 1)$:

$$\phi = 2\pi R_1, \ \theta = \arccos(\sqrt{R_2})$$

$$\begin{bmatrix} x \\ y \\ z \end{bmatrix} = \begin{bmatrix} \sin(\theta) \cdot \cos(\phi) \\ \sin(\theta) \cdot \sin(\phi) \\ \cos(\theta) \end{bmatrix} \tag{2}$$

This is represented in Fig. 6b.

The second step is to detect the location of the sun using a thresholding method. This is needed to align the center of the previously computed distribution (i.e. top of the hemispheric dome) to the actual sun location in the unit sphere. We choose a threshold of 240 in the red channel R of the RGB captured image, and compute the centroid of the largest area above the threshold ~~Savoy et al. (2016)~~(Savoy et al., 2016). We then compute the rotation matrix transforming the z-axis unit vector to the unit vector pointing towards the sky. We apply this rotation to all the sampled points, resulting in Fig. 6c.

This means that the amount of sampled points in a region of the hemisphere is proportional to the cosine of the angle between the sun direction and the direction to that region. We experimentally concluded that this achieves a good balance between all irradiance components. We thus consider the pixel values of 5000 points sampled using this method as input for the irradiance estimation.

3.2 Relative luminance calculation

For each of the i sampled pixels in the RGB image, we compute its luminance value using the following formula[1] ~~:~~. The formula is proposed in SMPTE Recommended Practice 177 (SMPTE, 1993). It is used to compute the luminance of an image from the *R*, *G* and *B* values of the *RGB* image.

$$Y_i = 0.2126 \cdot R_i + 0.7152 \cdot G_i + 0.0722 \cdot B_i$$

The JPEG compression format encodes images after applying a gamma correction. This non-linearity mimics the behavior of the human eye. This needs to be reversed in order to compute the irradiance. We use a gamma correction factor of 2.2, which is most commonly used in imaging systems ~~Poynton (2003)~~(Poynton, 2003). We thus apply the following formula, assuming pixel values normalized between 0 and 255:

$$Y_i' = 255(Y_i/255)^{2.2}$$

We then average the pixel values across all the i sampled points in the image, and denote it by $\mathcal{N}$. This pixel value given by $\mathcal{N} = (1/n)\sum_{i=1}^{n} Y_i'$, denotes the average luminance value of the sampled points from the image.

[1] ~~following SMPTE Recommended Practice 177~~

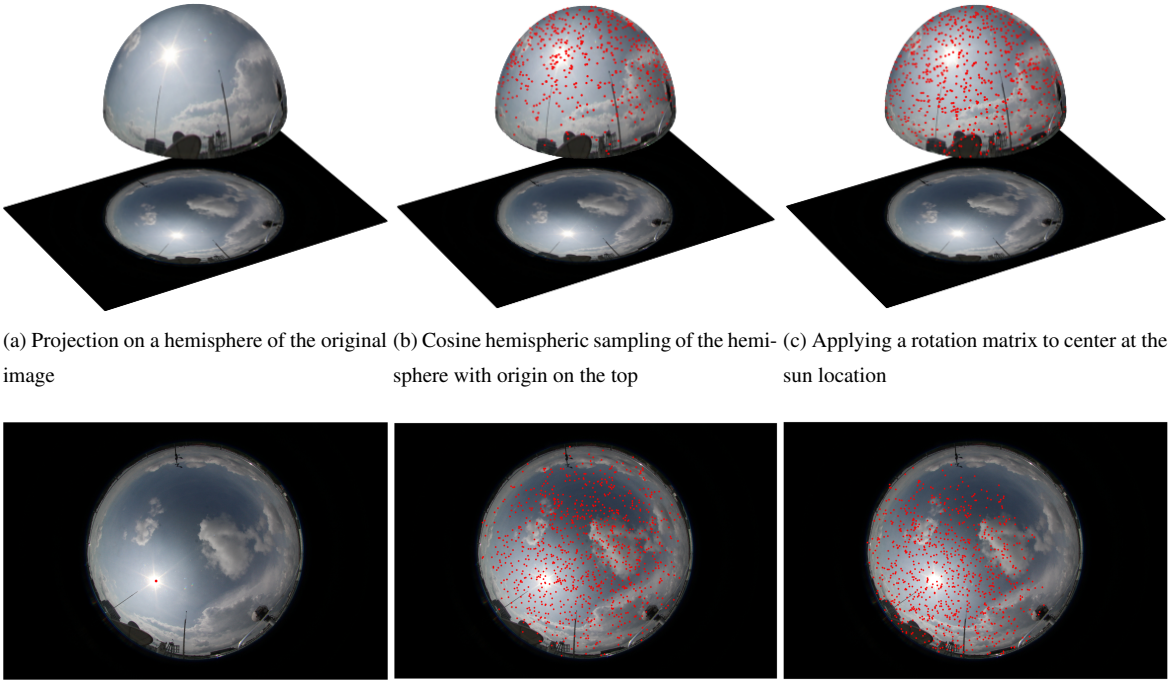

(a) Projection on a hemisphere of the original image

(b) Cosine hemispheric sampling of the hemisphere with origin on the top

(c) Applying a rotation matrix to center at the sun location

(d) Original image with detected sun location in red

(e) Projection on the image of the sampled points

(f) Projection on the image of the rotated sampled points

Figure 6. Cosine weighted hemispheric sampling process used to select the pixels used for solar irradiance estimation

However, each image of the sky camera is captured with varying camera parameters via ISO, F-number and shutter speed. These camera parameters can be read from the image metadata, and are useful to estimate the scene luminance. The amount of brightness of the sampled points $\mathcal{N}$, is proportional to the number of photons hitting the camera sensor. This relationship between scene luminance and pixel brightness is linear ~~Hiscocks and Eng (2011)~~(Hiscocks and Eng, 2011), and can be modeled using the camera parameters as:

$$\mathcal{N} = K_c \left(\frac{e_t \cdot S}{f_s^2} \right) \mathcal{L}_s$$

where $\mathcal{N}$ is the pixel value, K_c is a calibration constant, e_t the exposure time in seconds, f_s the aperture number, S the ISO sensitivity and $\mathcal{L}_s$ the luminance of the scene.

We can thus compute the relative luminance $\mathcal{L}_r$ using the following:

$$\mathcal{L}_r = \mathcal{N} \left(\frac{f_s^2}{e_t \cdot S} \right)$$

3.3 Modeling irradiance from luminance values

Using our hemispheric sampling and relative luminance computation, we therefore have one relative luminance value $\mathcal{L}_r$ per image. We propose our model using this relative luminance value to estimate the solar radiation. The usual sunrise time in Singapore is between 6:40 am and 7:05 am, and sunset time is approximately between 6:50 pm and 7:10 pm[1] ~~.~~. This information is obtained from (nea). Therefore, we consider images captured in the time interval of 7:00 am till 7:00 pm. We use our ground-based whole sky images captured during the time period from January 2016 till August 2016 to model the solar radiation. The solar irradiance is computed as the flux of radiant energy per unit area normal to the direction of flow. The first step in estimating irradiance from the luminance is thus to cosine weight it according to its direction of flow. We weight our measurements according to the solar zenith angle α. This is based on empirical evidences of our experiments on solar irradiance estimation. The modeled luminance $\mathcal{L}$ is expressed as:

$$\mathcal{L} = \mathcal{L}_r(\cos\alpha)$$

Let us assume that the actual solar radiation recorded by the weather station be $\mathcal{S}$. We check the nearest weather station measurement, for all the images captured by WAHRSIS between April 2016 till December 2016. Figure 7 shows the scatter plot between the image luminance and solar radiation. The majority of the data follows a linear relationship between the two. However, it deviates from linearity for higher values of luminance. This is mainly because of the fact that the mapping between scene luminance and obtained pixel value in the camera sensor becomes non-linear for large luminances. A more detailed discussion on this is provided in Section 5.

We ~~use a linear regressor~~ attempt to fit a linear model and other higher-order polynomial regressors to model the relationship between image luminance from sky camera images and the measured solar radiation. Figure 7 shows the best fit line for several orders of polynomial function. In order to provide an objective evaluation of the different models, we also compute the RMSE value between the actual- and regressed- values. Table 1 summarises the performance of the different order polynomials. We observe that lower order polynomials of degree 1 and 2 perform slightly inferior to those of higher order polynomials. We observe that the performance of cubic, quartic and quintic models are similar. However, from Fig. 7, we observe that the quartic and quintic models are highly ill-conditioned. Therefore, we choose the cubic model as our proposed model to model the measured solar radiation $\mathcal{S}$ from the image luminance $\mathcal{L}$. This is based on our assumption that the mapping from scene luminance to pixel values in the captured image is linear ~~. We also attempted using~~ for lower luminance values, and it behaves in a non-linear ~~model to model the relationship between image luminance and solar radiation; but we did not witness any improvement. Therefore, we used a linear model in our proposed framework.~~ fashion for higher luminance values. We use this selected model in all our subsequent discussions and evaluations.

We model solar radiation as~~: $\mathcal{S} = a \times \mathcal{L} + b$~~: $\mathcal{S} = a_3 \times \mathcal{L}^3 + a_2 \times \mathcal{L}^2 + a_1 \times \mathcal{L} + a_0$. The values of ~~$a$ and b~~ a_3, a_2, a_1 and a_0 are derived as ~~0.0138 and −39.896~~ $-4.25e-12$, $3.96e-07$, 0.00397 and 7.954 respectively for our data. Therefore, our proposed ~~model for~~ methodology in estimating solar irradiance from luminance is:

[1]

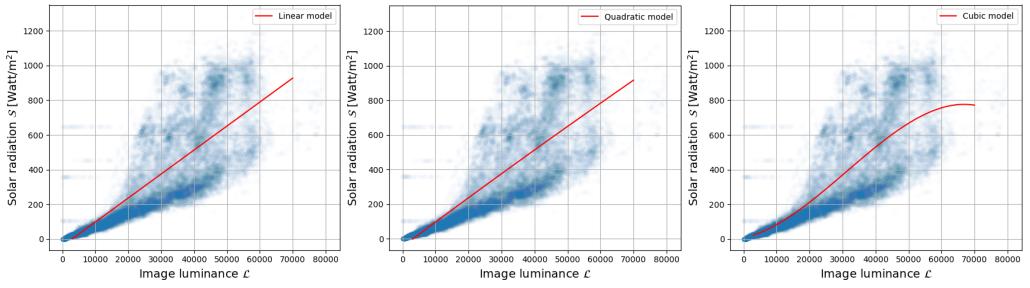

(a) Linear model (b) Quadratic model (c) Cubic model

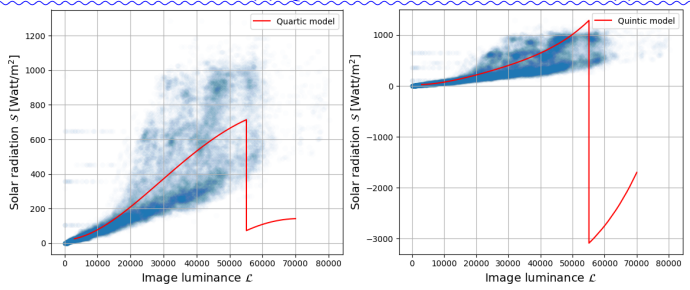

(d) Quartic model (e) Quintic model

Figure 7. ~~Model of the~~ Empirical fit between solar radiation ~~using the~~ and image luminance computed with our proposed framework. We observe that it deviates from linearity at higher luminance values. Also, the higher order polynomials are ill-conditioned.

Proposed models	**RMSE** (Watt/m^2)
Linear model (degree 1)	178.27
Quadratic model (degree 2)	178.26
Cubic model (degree 3)	176.57
Quartic model (degree 4)	176.52
Quintic model (degree 5)	176.49

Table 1. Performance evaluation of various polynomial order regressors. We measure the RMSE value for each of the models.

$$\mathcal{S} = 0.0138(-4.25e-12)\mathcal{L}^3 + (3.96e-07)\mathcal{L}^2 + (0.00397) \times \mathcal{L} - 39.896 + 7.954. \quad (3)$$

This model is derived specifically for equatorial region like Singapore, and the regression constants are based on our WAHRSIS sky imaging system. However, these values need to be fine-tuned while applying our methodology for other regions and different imaging system~~[1].~~. The source code of all the simulations in this paper is open-source, and the code repository is available online at https://github.com/Soumyabrata/estimate-solar-irradiance.

[1] ~~The source code of all the simulations in this paper is open-source, and the code repository is available online at Link to be updated here.~~

4 Performance Comparison and Validation

In this section, we evaluate the accuracy of our proposed ~~model. The model~~ approach. It is derived based on WAHRSIS images captured from January to August 2016. We also use these images to evaluate the accuracy of our proposed model. Furthermore, we benchmark our algorithm with other existing solar radiation estimation models.

4.1 Evaluation

One of the main advantages of our approach is that all rapid fluctuations of solar radiation can be accurately tracked from the image luminance. We illustrate this by providing the measured solar readings of 01-Sep-2016 in Fig. 8. The clear-sky model follows a cosine response and is shown in black; whereas the measured solar recordings is shown in red. We normalize our computed luminance in a manner ~~that~~ such that it matches the measured solar readings. We multiply each data points of the luminance with a conversion factor, such that the distance between corresponding inter-samples of luminance and weather station is minimized (cf. Appendix A for details). We use this normalization factor, in order to map the computed image luminance to follow the similar cosine clear sky model. We observe that our computed luminance from the whole-sky image and the measured solar radiation closely follows each other. We emphasize here that it is an important contribution to successfully track the rapid solar fluctuations. Unlike other solar estimation models based on meteorological sensor data, our proposed model can successfully estimate the *peaks* and *troughs* of solar readings accurately.

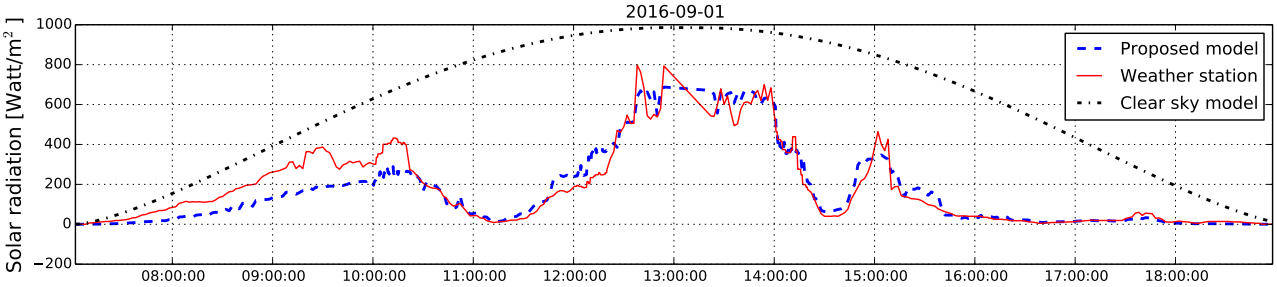

Figure 8. We show the measured weather station data (in red), and the clear sky radiation (in black) as on 01-Sep-2016. We observe that the image luminance normalized w.r.t. the measured solar radiation, follows the measured readings closely. The sampling interval between two measurements is 2 minutes.

Using our proposed methodology, we compute the luminance of all the captured images. We use Eq. 3, and estimate the corresponding solar radiation values. The ~~actual~~ estimated solar irradiance value is compared with the actual irradiance values obtained from the solar sensors. The actual ones are recorded in the collocated weather station. These recordings serve as the ground-truth measurements. Figure 9 shows the histogram of difference between the estimated and actual solar radiation. We observe that the estimated solar radiation do not deviate much from the actual solar radiation. It is clear that 47.9% of data points are concentrated in the range $[-100,+100]$ Watt/m^2.

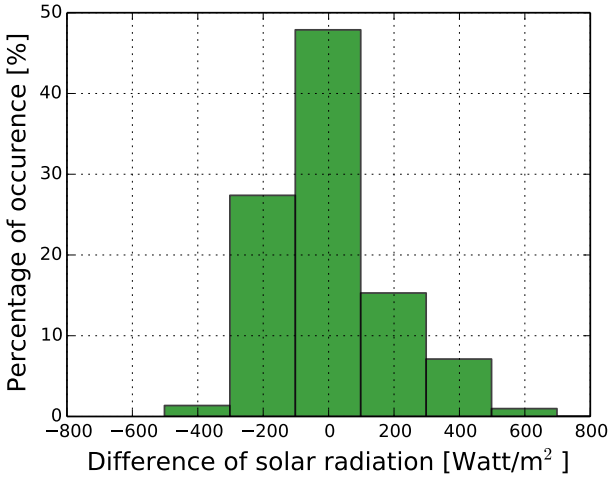

Figure 9. Histogram of difference between estimated and actual solar radiation. We observe that most of the data are concentrated in the 0-bin.

4.2 Benchmarking techniques

We benchmark our proposed approach with other existing solar estimation models. To the best of our knowledge, currently, there are no proposed models to estimate short-term fluctuations of solar irradiance from ground-based images. However, most remote sensing analysts have been using other meteorological sensor data eg. daily temperature, humidity, rainfall and dew point temperature to estimate daily solar irradiance. One of the pioneer work was done by Hargreaves and Samani ~~Hargreaves and Samani (1~~ who proposed a model based on daily temperature variations. Donatelli and Campbell ~~Donatelli and Campbell (1998)~~ (Donatelli and Campb the model by including clear sky transitivity as one of the factors. On the other hand, Bristow and Campbell ~~Bristow and Campbell (1984)~~ (B proposed a new model of solar radiation estimation, by including the atmospheric transmission coefficient. Subsequently, Hunt ~~et al. Hunt et al. (1998)~~ *et al.* (Hunt et al., 1998) showed that the solar estimation model can be further improved by incorporating the daily precipitation data in the model. We benchmark our proposed approach with these different existing models. We illustrate the various benchmarking models in Fig. 10. Unfortunately, most of these algorithms fail to capture the short-term variations of the actual solar radiation.

We calculate the Root Mean Square Error (RMSE) of the estimated solar radiation and Spearman's rank correlation coefficient as the evaluation metrics. The RMSE of an estimation algorithm represents the standard deviation of the actual and estimated solar radiation values. Table 2 shows the RMSE values of our proposed algorithm with the other existing benchmarking algorithms. Our proposed approach performs the best. We also evaluate the spearman correlation coefficients of the different benchmarking algorithms, since this is a non-parametric measure to find the relationship between measured and estimated solar radiation. This does not assume that the underlying dataset are derived from a normal distribution. We report the

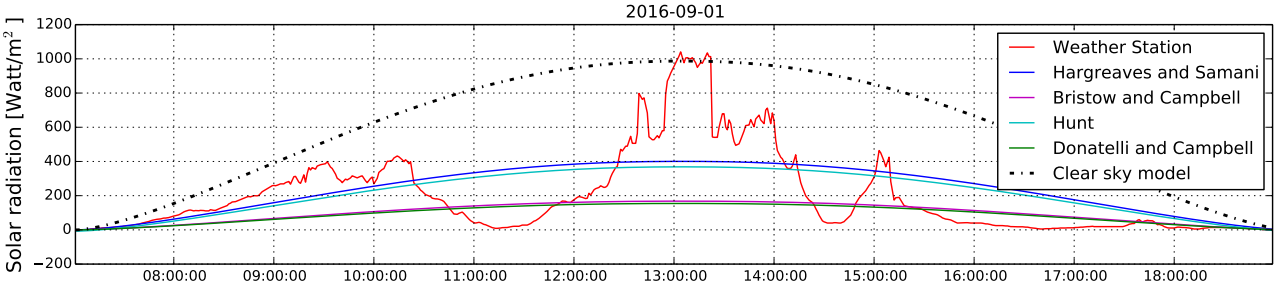

Figure 10. Comparison amongst different benchmarking solar estimation models, along with clear sky model and measured solar radiation on 01-Sep-2016. We observe most of the existing algorithms fail to capture the rapid fluctuations of the measured solar radiation.

correlation values in Table 2. Our proposed approach has also the highest correlation amongst all methods. Table 2 explains the results where the training and testing set of images are identical, and all images are considered for evaluation.

Methods	**RMSE** (Watt/m^2)	**Correlation**
Proposed approach	178.27	0.86
Hargreaves and Samani	982.35	0.67
Bristow and Campbell	318.07	0.68
Donatelli and Campbell	324.48	0.67
Hunt ~~et al.~~ *et al.*	922.66	0.65

Table 2. Benchmarking of our proposed approach with other solar radiation estimation models. All correlation values have p-value equal to 0.

Furthermore, we are also interested to check if our proposed model can generalize well with random samples of our captured sky camera images. We choose a random selection of images as the training set, and fit our linear regressor on these selected training images. The RMSE values are then calculated on these training images. We perform this analysis for varying percentage of training images. Each experiment is performed 100 times to remove any selection bias.

Figure 11(a) shows the results on training images. We observe that the variation of the RMSE values gradually decreases, as we increase the number of training images. Moreover, we also check the variation of RMSE values when the testing images are not identical as training images. Once we choose a random selection of images as training set, the remaining images are considered as the testing set. We show the RMSE results on such images in Fig 11(b). As expected, the variation of RMSE values increases with higher percentage of training images. The linear regressor model overfits the data, and provides higher variation in the error when tested on a fewer testing images. However, the average RMSE does not vary much in all cases. Therefore, our proposed model is free from selection bias, and generalizes well with random selection of training and testing images.

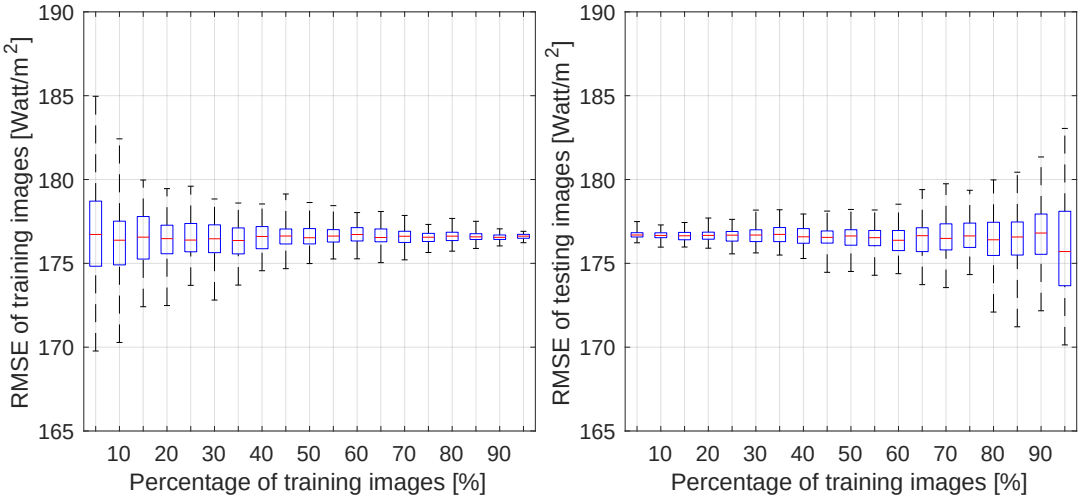

(a) Training images (b) Testing images

Figure 11. Effect of the percentage of training images on RMSE values. The lower and upper end of each box represents the 25^{th} and 75^{th} percentile of the data, and the red line represents the median value. Each experiment is conducted 100 times with a random choice of training and testing sets.

~~(a) Training images (b) Testing images Effect of the percentage of training images on RMSE values. The lower and upper end of each box represents the 25^{th} and 75^{th} percentile of the data, and the red line represents the median value. Each experiment is conducted 100 times with a random choice of training and testing sets.~~

We represent the scatter plot between the measured solar radiation and estimated solar radiation for the different benchmarking algorithms in Fig. 12.

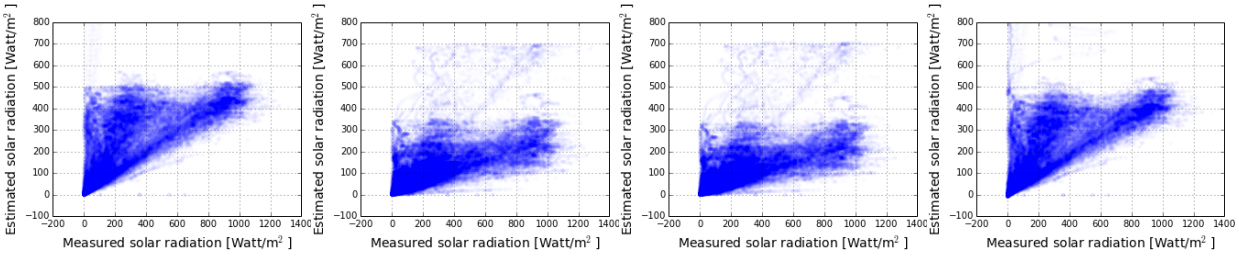

(a) Hargreaves and Samani (b) Bristow and Campbell (c) Donatelli and Campbell (d) Hunt *et al.*

Figure 12. Scatter plot between measured solar radiation and estimated solar radiation for the benchmarking algorithms.

We observe that there is no strong correlation for most of these existing algorithms. This is because meteorological sensor data alone, with no cloud information cannot determine the sharp fluctuations of the solar radiation. This is an important limi-

tation of these models, which we attempt to address in this paper. Our model based on sky images have additional information about cloud movement and its evolution, which is the fundamental reason behind rapid solar radiation fluctuations. In our proposed model, most of these short-term variations are captured properly (cf. Fig. 8).

~~(a) Hargreaves and Samani (b) Bristow and Campbell (c) Donatelli and Campbell (d) Hunt et al. Scatter plot between measured solar radiation and estimated solar radiation for the benchmarking algorithms.~~

5 Discussion

5.1 Short-term forecasts

Our proposed approach can estimate the solar radiation accurately with the least root mean square error, as compared to other models. The main advantage of our approach is that it can be used on predicted images as well, opening the potential for short term solar irradiance forecasting, which is needed in the solar energy field. As an initial case study, we have exploited optical flow techniques to estimate the direction and flow of cloud motion vectors between two successive image frames. We use the $(B-R)/(B+R)$ ratio channel of the sky/cloud image, where B and R are the blue and red channels respectively. We use an implementation of optical flow technique (flo) that uses a simpler conjugate gradient solver to obtain the flow field. Figure 13 illustrates the estimated flow field.

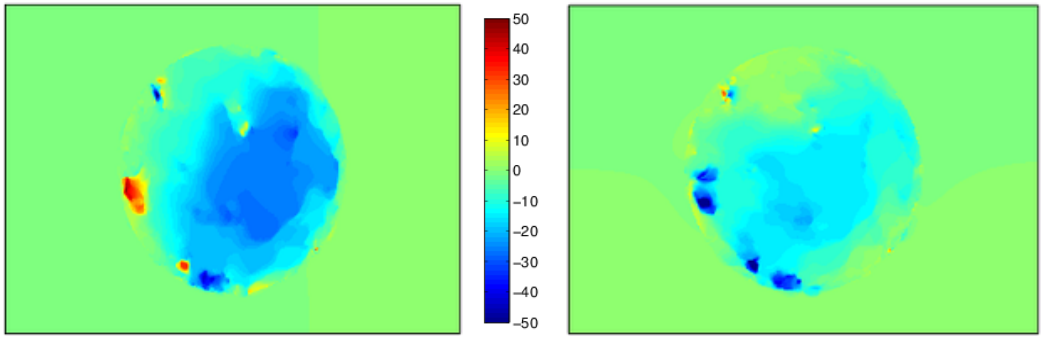

(a) Horizontal translation (b) Vertical translation

Figure 13. We visualize the horizontal and vertical translation of pixels between two successive frames, using optical flow technique.

Using the images captured at t and $t-2$ minutes, we estimate the horizontal- and vertical- translation of the pixels. Under the assumption that the flow of cloud motion vectors for the successive $t+2$ minutes is similar to that of previous frames, we estimate the future $t+2$ minutes frame, and subsequently the $t+4$ minutes frame. Figure 14 illustrates this. We obtain a forecast accuracy of 70% for a prediction lead time upto 6 minutes.

In the future work, we will use our proposed methodology of estimating solar irradiance on this predicted sky/cloud image. Such approach will provide us more stable and reliable forecasts of solar irradiance.

~~However, it suffers from a few drawbacks.~~

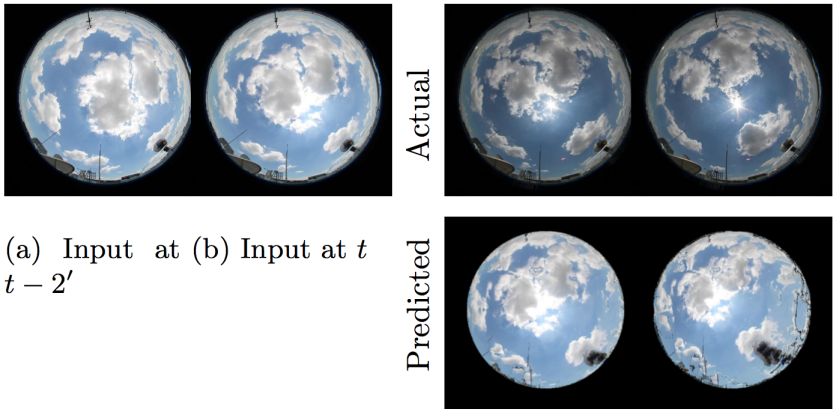

Figure 14. Prediction of sky/cloud image using optical flow technique.

5.2 Scope of improvement

This paper proposes an empirical model to estimate the solar irradiance from ground-based cameras. However, there are scopes of improvement in our approach. In this section, we highlight ~~them~~ the issues and suggest techniques to address them. Firstly, we use *JPEG* images instead of uncompressed *RAW* images for the computation of scene luminance. The *JPEG* compression algorithm introduces non-linearities in the pixel values and our proposed model thus deviates from a linear relationship. We can generate more consistent results by using only *RAW* format images. Nevertheless, we still use *JPEG* images, as they have a significantly smaller size and less perceptible distortion in image quality. This assumption is practical from an operational point of view. On the other hand, uncompressed *RAW* images have large file size and it is impossible to capture and store *RAW* images at short capturing intervals due to the induced latency. In our future work, we intend to use *RAW* format images for the computation of solar irradiance values from sky cameras.

Secondly, our captured images have a wide range of camera settings with varying shutter speed, ISO and aperture values. This is disadvantageous because the relationship between pixel value and camera aperture value becomes non-linear for larger F-numbers. The relationship deviates from linearity above F 4.0 ~~Hiscocks and Eng (2011)~~(Hiscocks and Eng, 2011). Figure 15 depicts the wide range of F-numbers in the captured images used in deriving our proposed model. We observe that a significant percentage of images have large F-numbers, where the non-linearity sets in. This can be solved by using the aperture priority mode of the sky camera, wherein the F-number is fixed, and the exposure time varies dynamically to match the lighting conditions of the scene.

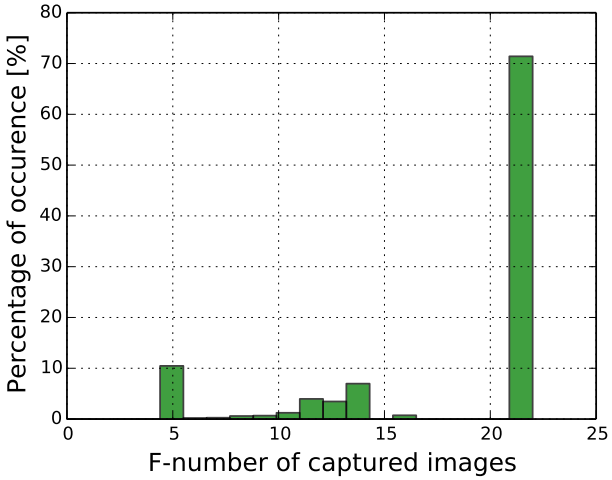

Figure 15. Distribution of F-number of the WAHRSIS images that are used to derive the proposed model.

6 Conclusion & Future work

We presented a method for estimating the rapid fluctuations of the solar irradiance using the luminance of images taken by a whole sky imager. We are able to estimate the sharp short-term variations, which significantly improves the state-of-the-art. This approach is of interest in the solar energy field, because these variations cause a sudden decrease in the electricity generation from solar panels. Short-term predictions of such ramp-downs are needed to maintain the stability of the power grid. Combining our solar irradiance estimation approach with cloud movement tracking in the input images could ultimately lead to better irradiance predictions. Such information on rapid fluctuations of solar irradiance can assist in establishing a high-reliability solar energy generation system. We also plan to explore methodologies from time-series modelling (Dev et al., 2018a), to predict solar irradiance.

7 Code availability

The source code of all simulations in this paper ~~will be made available online upon paper acceptance~~is available here: https://github.com/Soumyabrata/estimate-solar-irradiance.

Appendix A: Derivation of normalization factor

Let us suppose that $a_1, a_2, \ldots, a_t$ be the weather station records for t number of time stamps. The luminance values computed for each of the corresponding weather station points are represented by $b_1, b_2, \ldots, b_t$. We attempt to estimate the conversion factor x, such that the objective function $f(x)$ representing the inter-sample distances between weather station and computed luminance value is minimized.

We represent objective function $f(x)$ as:

$$f(x) = (xb_1 - a_1)^2 + (xb_2 - a_2)^2 + \ldots + (xb_t - a_t)^2$$
$$= \sum_{i=1}^{t} (xb_i - a_i)^2$$

We equate $f'(x)$ to 0, and the normalization factor x is found as $x = \frac{\sum_{i=1}^{t} a_i b_i}{\sum_{i=1}^{t} b_i^2}$.

Acknowledgements. This research is funded by the Defence Science and Technology Agency (DSTA), Singapore.

References

Optical Flow Matlab/C++ Code, https://people.csail.mit.edu/celiu/OpticalFlow/, accessed: 2019-08-09.

NEA | Weather, http://www.nea.gov.sg/weather-climate/forecasts, accessed: 2019-08-09.

Alonso-Montesinos, J. and Batlles, F. J.: The use of a sky camera for solar radiation estimation based on digital image processing, Energy, 90, Part 1, 377–386, 2015.

Alsadi, S. Y. and Nassar, Y. F.: Estimation of Solar Irradiance on Solar Fields: An Analytical Approach and Experimental Results, IEEE Transactions on Sustainable Energy, 8, 1601–1608, doi:10.1109/TSTE.2017.2697913, 2017.

Baharin, K. A., Abdul Rahman, H., Hassan, M. Y., and Gan, C. K.: Short-term forecasting of solar photovoltaic output power for tropical climate using ground-based measurement data, Journal of renewable and sustainable energy, 8, 053 701, 2016.

Bristow, K. L. and Campbell, G. S.: On the relationship between incoming solar radiation and daily maximum and minimum temperature, Agricultural and forest meteorology, 31, 159–166, 1984.

Chu, Y., Urquhart, B., Gohari, S. M., Pedro, H. T., Kleissl, J., and Coimbra, C. F.: Short-term reforecasting of power output from a 48 MWe solar PV plant, Solar Energy, 112, 68–77, 2015.

Dev, S., Savoy, F. M., Lee, Y. H., and Winkler, S.: WAHRSIS: A low-cost, high-resolution whole sky imager with near-infrared capabilities, in: Proc. IS&T/SPIE Infrared Imaging Systems, 2014.

Dev, S., Savoy, F. M., Lee, Y. H., and Winkler, S.: Design of low-cost, compact and weather-proof whole sky imagers for High-Dynamic-Range captures, in: Proc. International Geoscience and Remote Sensing Symposium (IGARSS), pp. 5359–5362, 2015.

Dev, S., Lee, Y. H., and Winkler, S.: Color-Based Segmentation of Sky/Cloud Images From Ground-Based Cameras, IEEE Journal of Selected Topics in Applied Earth Observations and Remote Sensing, PP, 1–12, 2016a.

Dev, S., Savoy, F. M., Lee, Y. H., and Winkler, S.: Estimation of solar irradiance using ground-based whole sky imagers, in: Proc. International Geoscience and Remote Sensing Symposium (IGARSS), pp. 7236–7239, 2016b.

Dev, S., Savoy, F. M., Lee, Y. H., and Winkler, S.: Estimation of solar irradiance using ground-based whole sky imagers, in: Proc. IEEE International Geoscience and Remote Sensing Symposium (IGARSS), pp. 7236–7239, IEEE, 2016c.

Dev, S., Savoy, F. M., Lee, Y. H., and Winkler, S.: Short-term prediction of localized cloud motion using ground-based sky imagers, in: Proc. IEEE TENCON, 2016d.

Dev, S., Wen, B., Lee, Y. H., and Winkler, S.: Ground-Based Image Analysis: A Tutorial on Machine-Learning Techniques and Applications, IEEE Geoscience and Remote Sensing Magazine, 4, 79–93, 2016e.

Dev, S., Manandhar, S., Lee, Y. H., and Winkler, S.: Study of clear sky models for Singapore, in: Progress in Electromagnetics Research Symposium-Fall (PIERS-FALL), 2017, pp. 1418–1420, IEEE, 2017.

Dev, S., AlSkaif, T., Hossari, M., Godina, R., Louwen, A., and van Sark, W.: Solar Irradiance Forecasting Using Triple Exponential Smoothing, in: 2018 International Conference on Smart Energy Systems and Technologies (SEST), pp. 1–6, IEEE, 2018a.

Dev, S., Savoy, F. M., Lee, Y. H., and Winkler, S.: High-dynamic-range imaging for cloud segmentation, Atmospheric Measurement Techniques, 11, 2041–2049, doi:10.5194/amt-11-2041-2018, https://www.atmos-meas-tech.net/11/2041/2018/, 2018b.

Donatelli, M. and Campbell, G. S.: A simple model to estimate global solar radiation, in: Proc. 5th European society of agronomy congress, pp. 133–134, 1998.

Feng, C., Cui, M., Hodge, B., Lu, S., Hamann, H., and Zhang, J.: Unsupervised Clustering-Based Short-Term Solar Forecasting, IEEE Transactions on Sustainable Energy, pp. 1–1, doi:10.1109/TSTE.2018.2881531, 2018.

Hargreaves, G. H. and Samani, Z. A.: Reference crop evapotranspiration from temperature, Applied engineering in agriculture, 1, 96–99, 1985.

Hiscocks, P. D. and Eng, P.: Measuring Luminance with a digital camera, Syscomp Electronic Design Limited, 2011.

Hunt, L. A., Kuchar, L., and Swanton, C. J.: Estimation of solar radiation for use in crop modelling, Agricultural and Forest Meteorology, 91, 293–300, 1998.

Huo, J. and Lu, D.: Comparison of cloud cover from all-sky imager and meteorological observer, Journal of Atmospheric and Oceanic Technology, 29, 1093–1101, 2012.

Jang, H. S., Bae, K. Y., Park, H., and Sung, D. K.: Solar Power Prediction Based on Satellite Images and Support Vector Machine, IEEE Transactions on Sustainable Energy, 7, 1255–1263, doi:10.1109/TSTE.2016.2535466, 2016.

Jiang, Y., Long, H., Zhang, Z., and Song, Z.: Day-Ahead Prediction of Bihourly Solar Radiance With a Markov Switch Approach, IEEE Transactions on Sustainable Energy, 8, 1536–1547, doi:10.1109/TSTE.2017.2694551, 2017.

Lautenbacher, C. C.: The global earth observation system of systems: Science serving society, Space Policy, 22, 8–11, 2006.

Lefèvre, M., Blanc, P., Espinar, B., Gschwind, B., Ménard, L., Ranchin, T., Wald, L., Saboret, L., Thomas, C., and Wey, E.: The HelioClim-1 Database of Daily Solar Radiation at Earth Surface: An Example of the Benefits of GEOSS Data-CORE, IEEE Journal of Selected Topics in Applied Earth Observations and Remote Sensing, 7, 1745–1753, 2014.

Lorenz, E., Hurka, J., Heinemann, D., and Beyer, H. G.: Irradiance Forecasting for the Power Prediction of Grid-Connected Photovoltaic Systems, IEEE Journal of Selected Topics in Applied Earth Observations and Remote Sensing, 2, 2–10, 2009.

Mueller, R., Dagestad, K.-F., Ineichen, P., Schroedter-Homscheidt, M., Cros, S., Dumortier, D., Kuhlemann, R., Olseth, J., Piernavieja, G., Reise, C., et al.: Rethinking satellite-based solar irradiance modelling: The SOLIS clear-sky module, Remote sensing of Environment, 91, 160–174, 2004.

Ouarda, T. B. M. J., Charron, C., Marpu, P. R., and Chebana, F.: The Generalized Additive Model for the Assessment of the Direct, Diffuse, and Global Solar Irradiances Using SEVIRI Images, With Application to the UAE, IEEE Journal of Selected Topics in Applied Earth Observations and Remote Sensing, 9, 1553–1566, 2016.

Pagano, T. S. and Durham, R. M.: Moderate resolution imaging spectroradiometer (MODIS), in: Proc. Sensor Systems for the Early Earth Observing System Platforms, vol. 1939, pp. 2–17, International Society for Optics and Photonics, 1993.

Poynton, C.: Digital Video and HDTV Algorithms and Interfaces, Morgan Kaufmann Publishers Inc., 2003.

Rizwan, M., Jamil, M., and Kothari, D. P.: Generalized Neural Network Approach for Global Solar Energy Estimation in India, IEEE Transactions on Sustainable Energy, 3, 576–584, doi:10.1109/TSTE.2012.2193907, 2012.

Savoy, F. M., Dev, S., Lee, Y. H., and Winkler, S.: Geo-referencing and stereo calibration of ground-based whole sky imagers using the sun trajectory, in: Proc. International Geoscience and Remote Sensing Symposium (IGARSS), 2016.

Scaramuzza, D., Martinelli, A., and Siegwart, R.: A toolbox for easily calibrating omnidirectional cameras, in: Proc. IEEE/RSJ International Conference on Intelligent Robots and Systems, pp. 5695–5701, IEEE, 2006.

Shakya, A., Michael, S., Saunders, C., Armstrong, D., Pandey, P., Chalise, S., and Tonkoski, R.: Solar Irradiance Forecasting in Remote Microgrids Using Markov Switching Model, IEEE Transactions on Sustainable Energy, 8, 895–905, doi:10.1109/TSTE.2016.2629974, 2017.

Silva, A. A. and Souza-Echer, M. P.: Ground-based observations of clouds through both an automatic imager and human observation, Meteorological Applications, 23, 150–157, 2016.

SMPTE, R.: RP 177-1993, Derivation of Basic Television Color Equations, 1993.

Yang, D. and Chen, N.: Expanding Existing Solar Irradiance Monitoring Network Using Entropy, IEEE Transactions on Sustainable Energy, 6, 1208–1215, doi:10.1109/TSTE.2015.2421734, 2015.

Yang, D., Jirutitijaroen, P., and Walsh, W. M.: The estimation of clear sky global horizontal irradiance at the equator, Energy Procedia, 25, 141–148, 2012.

Yuan, F., Lee, Y. H., Meng, Y. S., and Ong, J. T.: Water Vapor Pressure Model for Cloud Vertical Structure Detection in Tropical Region, IEEE Transactions on Geoscience and Remote Sensing, 54, 5875–5883, 2016.